International Journal of Thin Films Science and Technology

http://dx.doi.org/10.18576/ijtfst/050111

The Effects of Plasma Foucing Shots on Structural and Optical Properties of ZnTe Thin Films

G. El-Kashef *

Plasma and Nuclear Fusion Department, Nuclear Research Center, Atomic Energy Authority, Egypt

Received: 15 Oct. 2015, Revised: 20 Nov. 2015, Accepted: 25 Nov. 2015.
Published online: 1 Jan. 2016.

Abstract: Zinc telluride (ZnTe) thin film was deposited onto glass substrates in terms of the thermal evaporation technique. The experiments XRD of both powder and thin films of ZnTe showed that the films are polycrystalline and have a zinc blende (cubic) structure. Thin films of the same thickness have been exposed to plasma focusing (PF) with 0, 5, 10 and 15 shots. The structure. It is observed that the increasing in the number of PF shots can reduce crystallize size and increase the microstrain of ZnTe thin film. It is also observed that the the increasing in the number of PF shots can effectively improve the transmission spectra of the samples particularly in medium and transparent regions, therefore the refractive index decrease. It is observed that the increasing number of PF shots causes decreasing in optical band gap.

Keywords: Zinc telluride; thin film, PF shots, refractive index; Optical band gap.

PACS: *61.05.cp*, 52.40.Hf, 42.50.Nn

1 Introduction

ZnTe has zinc-blend structure with a lattice constant of 6.104 Ǻ, and is one of the promising II–VI materials for pure green lightemitting diodes, solar cells, and terahertz detectors [1-3]. Zinc telluride is an important semiconducting material for the development of various modern solid state devices (blue light emitting diodes, laser diodes, solar cells, microwave devices, etc.) It is a direct band gap semiconductor having band gap 2.26 eV at 300 K and usually a p-type semiconductor. It has potential applications in electronic and optical devices [4-6]. Moreover, the optical properties are closely related to the structure of the films and study of the optical properties gives valuable information about the ZnTe properties. The effects of ions, electrons, and other energetic particles are now widely utilized for substrate cleaning as well as to assist and control film growth. Some of the particles are not just assisting but they may condense and thereby become part of the growing film [7]. The role of nitrogen plasma-surface reactions is very important in various phenomena of technological interest such as corrosion, surface functionalization, and thin film growth. There is a number of plasma process parameters which could affect the resulting properties of the treated surface such as electrode temperature, plasma pressure, rf plasma processing power, rf plasma processing time, etc. One of the most effective parameters is the plasma processing power. The amount of power applied to a plasma system affects several plasma parameters such as electrode temperature. As power increases, greater ion energies are obtained further enhancing etching due to ion bombardment [8, 9]. In the present work, we studied the effect of plasma focusing shots on structural and optical properties of ZnTe thin films.

2 Experimental

Zinc Telluride (ZnTe) powder of "Aldrich Chemical Co." make having purity of >99.999% was used. The glass thin films were deposited by evaporating Zinc Telluride (ZnTe) from a resistance heating quartz glass crucible onto clean glass substrates kept at room temperature, using a conventional coating unit (Denton Vacuum DV 502 A) and a vacuum of about 2x 10^{-6} Torr. The evaporation rate as well as the film thickness was controlled using a quartz crystal DTM 100 monitor. The mechanical rotation of the substrate holder (≈ 30 rpm) during deposition produced homogeneous film. The temperature rise of the substrate owing to radiant heating from crucible was negligible. Small fluctuations in the measured transmittance (≈ 1.0 %) of studied films confirm their homogeneity. The mechanical rotation of the substrate holder was about ≈30 rpm during deposition produced in order to raise the homogeneity of film. Both the deposition rate and the film thickness were controlled using

*Corresponding author E-mail: gmelkashef@gmail.com

a quartz crystal monitor DTM 100. The deposition rate was maintained 20 Å/s during the sample preparations. The experimental setup of the present plasma focusing device is shown in fig. 1.

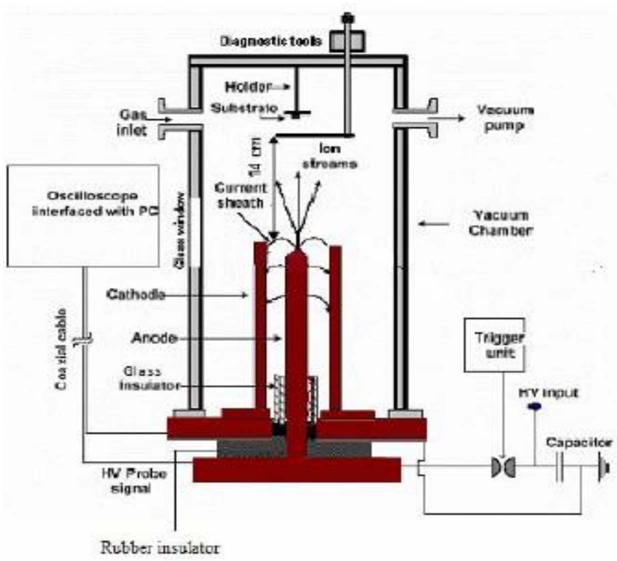

Fig. 1: Schematic of experimental setup for PF device.

The system is energized by a capacitor bank consists of four capacitor which are connected in parallel and has a total capacitance of 30.84 μf and charged up to 8 KV giving a peak discharge current up to 150 kA. To initiate the discharge through the electrodes a high voltage trigger was located near the spark gap which is a vital element since it is responsible to start the breakdown just before the shots. The cleaning process of the spark gap is carried out before and after 5 shots. The discharge chamber is made of stainless steel and has a length of 40 cm and diameter of 38 cm. Moreover, the electrodes of the plasma focus device in this experiment are a solid cylindrical tube to a void the excessive hard x-ray emission from the anode surface due to electron bombardment. The plasma focus is operated with argon as the working gas. The device was evacuated to lower than 10^{-2} Pa before puffing Argon gas by rotary van pump) and filled with the required gas (argon) to a particular pressure (0.2–2 Pa) before operation. This level of vacuum proved to be sufficient for operating with good focus in argon gas. The structure of the prepared powder and thin films were examined by XRD analysis (Philips X-ray diffractometry (1710)) with Ni-filtered Cu Kα radiation with λ = 0.15418 nm).The intensity data were collected using the step scanning mode with a small interval (Δ2θ=0.02º) with a period of 5 s at each fixed value to yield reasonable number of counts at each peak maximum. The transmittance measurements were carried out using a double-beam (Jasco V670) spectrophotometer, at normal incidence of light and in a wavelength range between 300 and 2500 nm. Without a glass substrate in the reference beam, the measured transmittance spectra were used in order to calculate the refractive index and the film thickness of ZnTe thin films according to Swanepoel's method.

3 Results and Discussion

Fig. 2 shows the X-ray diffractogram of ZnTe powder according to (JCPDS Data file: 01-0582-cubic), which exhibit a polycrystalline nature.

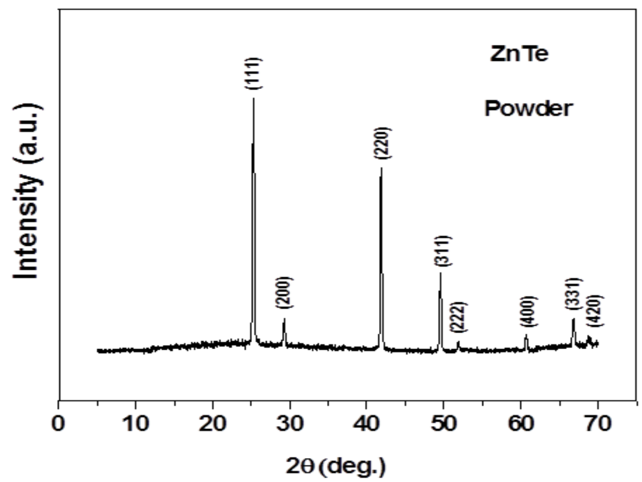

Fig. 2: X-ray diffraction spectra of ZnTe powder

Fig. 2 illustrates the XRD patterns of ZnTe thin films of different rf plasma process power at 300, 400, 500 W. This figure shows that the X-ray diffraction (XRD) analysis of ZnTe, that revealed that the films are polycrystalline of zinc-blende structure with peaks at 2θ = 25.42º, 42.20º and 49.87º corresponding to C(1 1 1), C(2 2 0) and C(3 1 1) orientations, respectively (JCPDS Data file: 01-0582-cubic). Fig. 2 also displays that the intensity of the peak decreases with increasing the number of PF shots. This figure shows that the intensity peaks are broader than the as deposited sample. The broadened in XRD thin film peaks are due to instrumental and microstructure parameters (crystallite size and lattice strains) [10]. The pure line profile is extracted by deconvoluting the instrumental broadening factor from the experimental line profile. The pure line profile can be used for calculating the microstructure parameters, crystallite size and microstrain. In this work, the instrumental broadening-corrected of pure breadth of each reflection was calculated from the parabolic approximation correction [10]:

$$\beta(2\theta) = \sqrt{\beta_{obs}^2 - \beta_{ref}^2} \quad \text{(rad)} \qquad (1)$$

Where β_{abs} and β_{ref} are the breadth (in radians) of the same Bragg-peak from the XRD scans of the experimental and reference powder, respectively. The reference powder was of ZnTe annealed at 300 °C for 2 h. The breadth decreases at each reflection with increasing the number of PF shots for ZnTe thin films. The method that based on the separation of crystallite size and strain takes the following form [11]:

$$\beta(2\theta)\cos\theta_0 = \frac{\lambda}{D_v} + 4e\left(\sin\theta_0\right) \qquad (2)$$

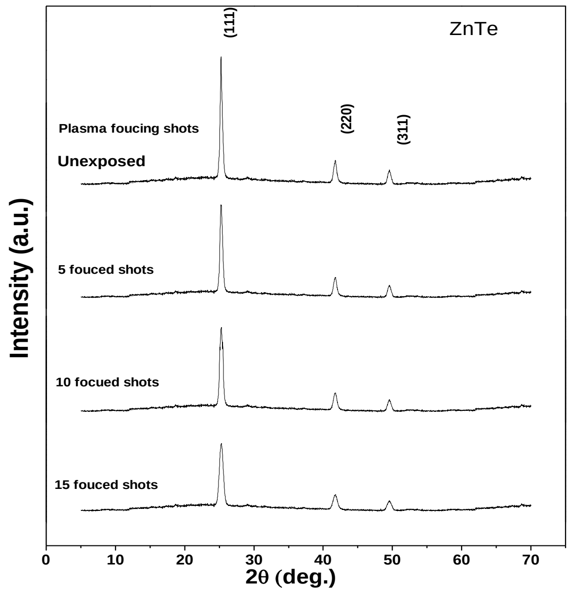

Fig. 3: XRD pattern of unexposed and exposed for 5, 10 and 15 plasma focusing shots of ZnTe thin films.

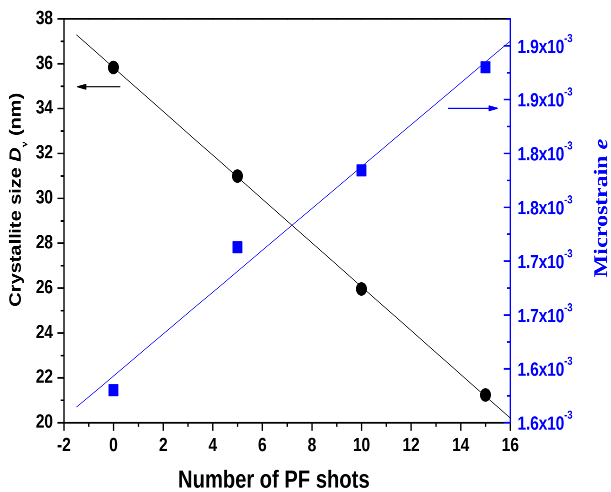

Fig. 4: Crystallite size and lattice strain separation calculating using $\beta(2\theta)\cos(\theta_0)$ versus *sin(θ₀)* according to "Williamson Hall" method for for of unexposed and exposed for 5, 10 and 15 plasma focusing shots of ZnTe thin films.

Fig. 4 shows a (*Dv*) and (*e*) of rf plasma process power of ZnTe thin films. It is observed that the (*Dv*) decreases with increase the number of PF shots but *(e)* exhibited an opposite behavior. This behavior may be attributed to the increase in lattice defects among the grain boundary due to presence of argon atoms, which increase with increasing the number of PF shots.

Fig. 4 shows the transmittance for unexposed and exposed for 5, 10 and 15 shots of ZnTe thin films. This figures show that the transmittance is drastically improved by increasing the number of PF shots and the extremes of interference shifted towards the lower wavelengths. Swanepoel's method [12] has been employed extensively by many researchers [12-16], to calculate the refractive index and thickness of the thin films. Swanepoel's method based on a creation of top and bottom envelopes to the interference maxima and minima observed in transmittance spectra as shown for example Fig. 5.

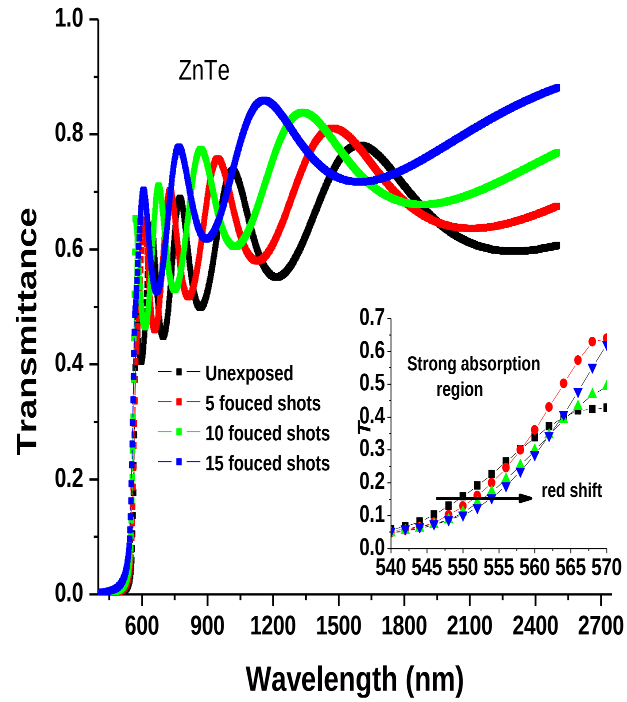

Fig. 5: Typical transmittance spectra for of unexposed and exposed for 5, 10 and 15 plasma focusing shots of ZnTe thin films. The inset shows the shift in strong absorption region.

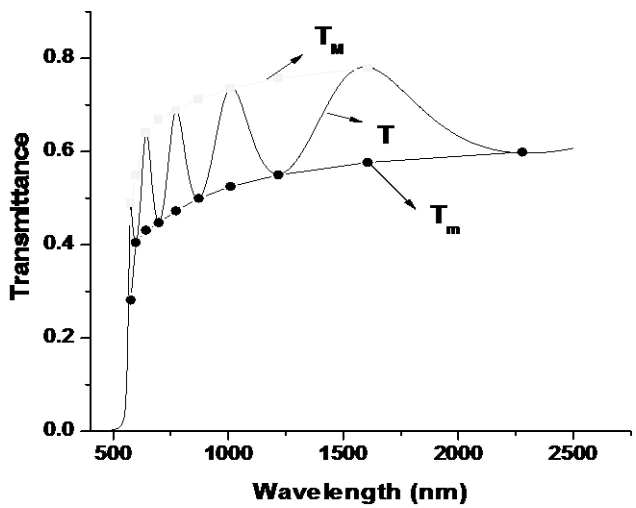

Fig. 6: The typical transmission spectra for as deposited ZnTe thin film.Curves T_M, T_m, according to the text.

The value of the refractive index of the film ***n***, in the spectral region of medium and weak absorption, can be calculated by the expression

$$n_1 = \left[N_1 + (N_1^2 - s^2)^{\frac{1}{2}} \right]^{\frac{1}{2}} \tag{3}$$

Where

$$N_1 = 2s\frac{T_M - T_m}{T_M T_m} + \frac{s^2+1}{2}$$

Here T_M and T_m, are the transmission maximum and the corresponding minimum at a certain wavelength λ. Alternatively, one of these values is an experimental interference extreme and the other one is derived from the corresponding envelope; both envelopes were computer-generated using the origin version 7 program using more than one procedure. On the other hand, the necessary values of the refractive index of the substrate are obtained from the transmission spectrum of the substrate, T_s using the well-known equation [17]:

$$s = \frac{1}{T_s} + (\frac{1}{T_s} - 1)^{\frac{1}{2}} \tag{4}$$

. Moreover, if n_{el} and n_{e2} are the refractive indices at two adjacent maxima (or minima) at λ_1 and λ_2, it follows that the film thickness is given by the expression

$$d = \frac{\lambda_1 \lambda_2}{2(\lambda_1 n_{e2} - \lambda_2 n_{e1})} \tag{6}$$

The values of *d* of different samples determined by this equation. Fig. 7 shows the reduction of film thickness of ZnTe thin films as the the function of plasma process power.

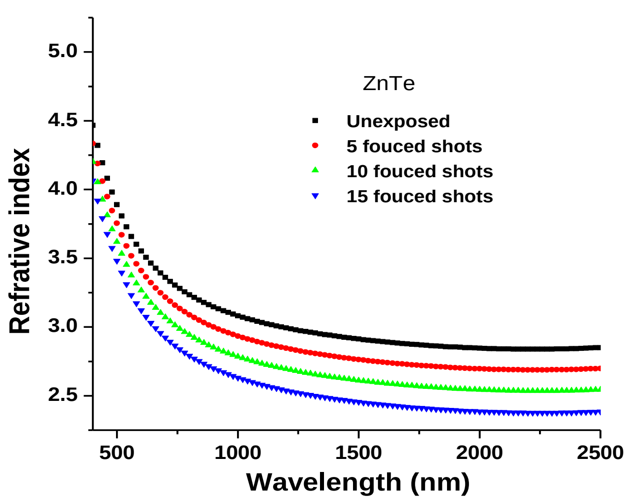

Fig. 7: Refractive index dispersion spectra of unexposed and exposed for 5, 10 and 15 plasma focusing shots of ZnTe thin films.

The improvement of refractive transmittance leads to a decrease in refractive index in comparable with the refractive index of as deposited sample may be attributed to the reduction of film thickness as a result of the decrease of film thickness due to an increasing the number of PF shots.

Since the values of the refractive index are already known from the Cauchy dispersion equation as shown in Fig. , the absorbance $x_a(\lambda)$ can be calculated from the interference-free transmission curve using the well-known equation, often used in optical studies, proposed by Connell and Lewis [18]

$$x_a = \left\{ P + \left[P^2 + 2QT_\alpha(1 - R_2R_3) \right]^{\frac{1}{2}} \right\} / Q \tag{7}$$

Where

$$P = (R_1-1)(R_2-1)(R_3-1)$$

And

$$Q = 2T_\alpha(R_1R_2 - R_1R_3 - 2R_1R_2R_3)$$

and R_1 , R_2, and R_3, the reflectances of the air-film, film-substrate and substrate-air interfaces: $R_1 = [(1 - n)/(1 + n)]^2$, $R_2 = [n - s)/(n + s)]^2$ and $R_3 = [(s - 1)/(s + 1)]^2$, respectively. For $\alpha \leq 10^5$ cm^{-1}, the imaginary part of the complex index of refraction is much less than *n*, so that the previous expressions to calculate the reflectance are valid. In the region of strong absorption the interference fringes disappear, in other words, for very large α the three curves T_M and T_m, converge to a single curve. Moreover, since d is also known, the relation $x_a = \exp(-\alpha d)$ can then be solved and thus, the values of the absorption coefficient are derived. In order to complete the calculation of the optical constants, the extinction coefficient is estimated from the values of α and λ using the already mentioned formula $k = \alpha\lambda/4\pi$. **Figure 8** illustrates the dependence of *k* on wavelength for the as for unexposed and exposed for 5, 10 and 15 shots of ZnTe thin films.

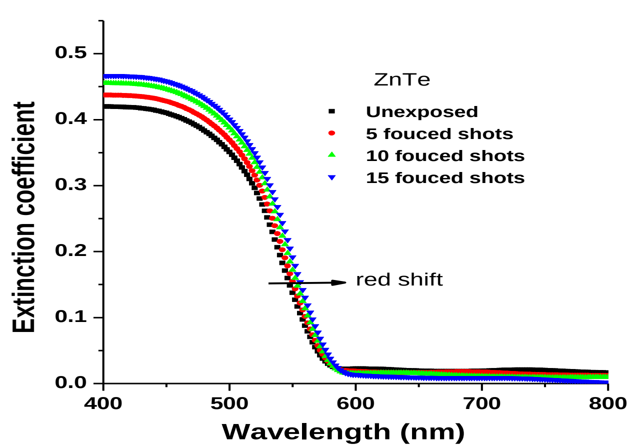

Fig. 8: The extinction coefficient versus wavelength of unexposed and exposed for 5, 10 and 15 plasma focusing shots of ZnTe thin films.

Finally, the optical hand gap will be found from the calculated values of α to that end, it should be pointed out that the absorption coefficient of amorphous semiconductor.

The vicinity of the fundamental absorption edge, for allowed direct band-to-band transitions, neglecting exciton effects, the absorption coefficient is described by the

$$\alpha(h\upsilon) = \frac{K(h\upsilon - E_g^{opt})^p}{h\upsilon} \quad (8)$$

where K is a characteristic parameter for respective transitions [19], $h\nu$ denotes photon energy, E_g^{opt} is optical energy gap and p is a number which characterizes the transition process. Different authors [13,15,20] have suggested different values of p for different glasses, $p = 2$ for amorphous semiconductors (indirect transition) and $p = 1/2$ for crystalline semiconductor (direct transition). In the case of different thickness of polycrystalline of ZnTe thin films the direct transition is valid. **Fig. 9** shows a typical best fit of $(\alpha h\nu)^2$ versus photon energy (hν) for for unexposed and exposed for 5, 10 and 15 shots of ZnTe thin films.

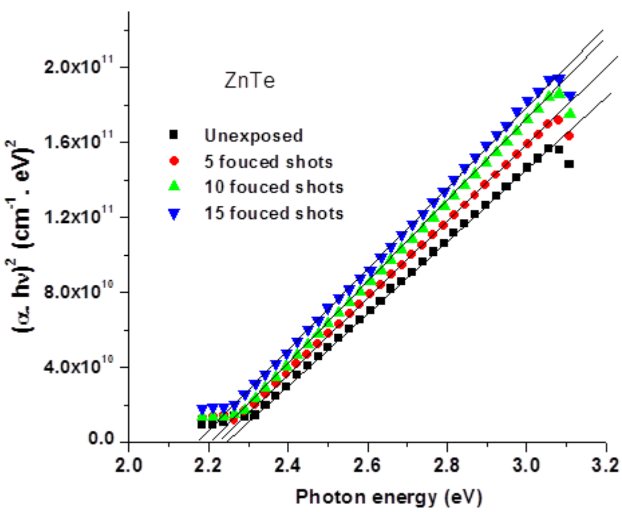

Fig. 9: The dependence of $(\alpha h\nu)^{1/2}$ on photon energy $h\nu$ for the four samples for of unexposed and exposed for 5, 10 and 15 plasma focusing shots of ZnTe thin films.

The values of the direct optical band gap E_g^{opt} were taken as the intercept of $(\alpha h\nu)^2$ vs. $(h\nu)$ at $(\alpha h\nu)^2 = 0$ for the allowed direct transition. The estimated values of E_g^{opt} in for unexposed and exposed for 5, 10 and 15 shots of ZnTe thin films are shown in Fig. 10. The optical band gap decrease with increasing the number of PF shots. The decrease of E_g^{opt} for direct transition may be attributing to the decrease in both crystallites size and film thickness.

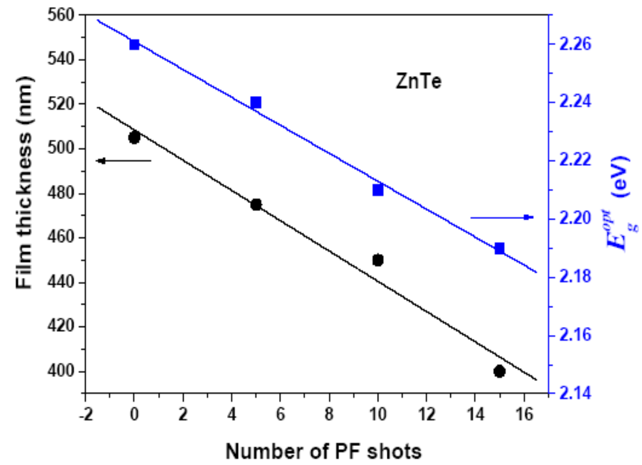

Fig. 10: Film thickness and optical band gap as a function of number of PF shots.

4 Conclusions

Zinc telluride (ZnTe) thin films were deposited onto glass substrates in terms of the thermal evaporation technique. The experiments XRD of powder, for unexposed and exposed for 5, 10 and 15 shots of ZnTe thin films showed that the films are polycrystalline and have a zinc blende (cubic) structure. The calculated microstructure parameters of the ZnTe thin films such as crystallite size (D_v) and microstrain e showed that the size of crystallites decrease with increasing the number of PF shots of ZnTe thin films, while the microstrain shows an opposite variation trend due to the increase in lattice defects, which were pronounced at higher value of PF shots (15). Swanepoel's method has been applied in terms of transmittance spectra for unexposed and exposed for 5, 10 and 15 shots of ZnTe thin films to determine the refractive index and average thickness of the films. It is also observed that for unexposed and exposed for 5, 10 and 15 shots of ZnTe thin films can effectively improve the transmission spectra of the samples particularly in medium and transparent regions, therefore the refractive index decrease. The optical constants and energy gap of for unexposed and exposed for 5, 10 and 15 shots of ZnTe thin films have been determined The increase of E_g^{opt} for direct transition may be also attributing to the decrease in crystallites size and film thikness.

References

[1] W. B. Jensen, *Journal of chemical education* **74** (1997), p. 1063.

[2] M. P. Valkonen, S. Lindroos, M. Leskela and *Appl. Surf. Sci.* **134** (1998), p. 283.

[3] I. T. Sinaoui, F. Chaffar Akkar, F. Aousgi and M. Kanzari, *Int. J. Thin Fil. Sci. Tec.* **3, No. 1** (2014), p. 19.

[4] Y. Ni, G. Yin, J. Hong and Z. Xu, *Mater. Res. Bull* **39** (2004),

p. 1967.

[5] K. C. Bhahada, B. Tripathi, N. K. Acharya, P. K. .Kulriya and Y. K. Vijay, *Applied Surface Science* **255** (2008), p. 2143.

[6] G. I. Rusu, P. Prepelita, R. S. Rusu, N..Apetroaie, G. Oniciuc and A. Amariei, **8(3)** (2006), p. 922.

[7] A. Anders and 200, *Surf. Coat. Technol.* **200** (2005), p. 1893.

[8] S. Salimian, C.B. Cooper and M. E. Day, *J. Vac. Sci.Technol. B* **5** (1987), p. 1606.

[9] K. D. Allen, H.H. Sawin and A. Yokozeki, *J. Electrochem. Soc.* **133** (1986), p. 2331.

[10] X. Mathew, J.P. Enriquez, P. Sebastian, M. Pattabi, A. Sanchez-Juarez, J. Campos, J.C. McClure and V.P. Singh, *Sol. Energy Mater. Sol. Cells* **63** (2000), p. 355.

[11] G. K. Williamson and H. W. H., *Acta Metallurgica* **1** (1953), p. 22.

[12] R. Swanepoel, *J. Phys. E: Sci. Instrum.* **17** (1984), p. 896.

[13] E. Márquez, J.M. González-Leal, A.M. Bernal-Oliva, R. Jiménez-Garay and T. Wagner, *Journal of Non-Crystalline Solids* **354** (2008), p. 503.

[14] E. R. Shaaban, *Mater. Chem. Phys.* **100** (2006), p. 411.

[15] J.M. Gonzalez-Leal, R. Prieto-Alcon, J.A. Angel and E. Marquez, *J. Non-Cryst. Solids* **315** (2003), p. 134.

[16] M. El-Hagary, M. Emam-Ismail, E. R. Shaaban and I. Shaltout, *J. Alloy Comp.* **485** (2009), p. 519.

[17] T. S. Moss, *Optical Properties of Semiconductors (London: Buttenvorths)* (1959).

[18] G. A. N. Connell and A. J. Lewis, *Phys. Status Solidi b* **60** (1973), p. 291.

[19] J. I. Pankove, *Optical Processes in Semiconductors Dover, New York* (1977), p. 44.